Polar Meteorol. Glaciol., **12**, 130–139, 1998

EXPERIMENTAL STUDY ON LIGHT SCATTERING FROM AN ARTIFICIAL ICE CLOUD

Yoshiaki SASAKI[1], Naoki NISHIYAMA[2] and Yoshinori FURUKAWA

Institute of Low Temperature Science, Hokkaido University, Kita-ku, Sapporo 060-0819

Abstract: A new experimental system was developed to clarify the relationship between the optical properties of an ice cloud and the physical properties (*e.g.*, shapes of ice crystals) of ice crystals in the cloud. An artificial ice cloud was formed in a cloud chamber which was set up in a cold laboratory, and the scattering intensity of laser light (wavelength of 633 nm) scattered by ice clouds was measured as a function of scattering angle. The ice crystals were simultaneously observed during the light scattering measurements. In this paper, we discuss the relationships between the light scattering properties of ice clouds and the shapes of ice crystals, which are one component of the physical properties of ice cloud.

1. Introduction

The angular distributions of light scattering intensities of ice clouds such as cirrus clouds are of great importance for the quantitative treatment of radiation transfer through the atmosphere and for the estimation of a thickness and a height of cirrus cloud by satellite-based remote sensing (LIOU, 1992). However, the angular distributions are strongly affected by physical properties of the ice crystals, such as their shapes, size distributions, fall orientations, spatial concentrations, and so on. Consequently, it is necessary to clarify how the physical properties of ice cloud affect the angular scattering intensity of the ice clouds.

Since the 1980s, computer simulations have been used to clarify the relationships between the optical properties of ice clouds and the physical properties of ice crystals in the clouds (WENDLING *et al.*, 1979; ROCKWITZ, 1989; TAKANO and LIOU, 1989a, b). In these simulations, the light scattering properties of ice clouds consisting of hexagonal solid columns or plates have been calculated. Recently, MACKE (1993), and TAKANO and LIOU (1995) have succeeded in simulating light scattering from ice crystals with irregular shapes, such as hollow columns, bullet rosettes and dendritic plates. They showed that the scattering patterns for the irregular shaped ice crystals are different from those for simple hexagonal solid columns or plates. However, it is still impossible to carry out computer simulations for particles with a more complex shape, such as combination bullets, crossed plates and so on (HEYMSFIELD and KNOLLENBERG, 1972; HEYMSFIELD, 1975).

[1]Present address: National Research Institute for Earth Science and Disaster Prevention, 3–1 Tennodai, Tsukuba 305-0006.

[2]Present address: Japan Weather Association, Sapporo Branch, Chuo-ku, Sapporo 064-0824.

Consequently, it is important to clarify the relationships between the scattering patterns and the physical structures of crystals by well-controlled laboratory experiments. Although some experimental studies have been carried out (MORITA, 1973; NIKIFORVA *et al.*, 1977; SASSEN and LIOU, 1979a, b), there are still many ambiguous points concerning these relationships. The main reason for this is the difficulty of simultaneously measuring the scattering intensity and the physical properties of ice crystals.

In this work, we constructed a new experimental apparatus to make artificial ice-clouds, and we simultaneously observed the total light scattering and the shapes of ice crystals, which are one component of the physical properties of ice crystals. Analyzing these results, we discuss the light scattering properties of clouds in relation to the shapes of ice crystals through a comparison of the simulation results.

2. Experimental Method

2.1. Experimental apparatus

Figure 1a shows a vertical cross-section of the experimental system that was used for measuring scattering intensity in the horizontal scattering plane. The system consists of a cloud chamber (1 m×1 m×1 m in volume), a glass cylinder (0.15 m in diameter), an optical system for the measurement of scattering patterns, and a microscope under the glass cylinder. Experiments using this apparatus were conducted in a cold laboratory at a temperature of −20°C.

Experiments were carried out according to the following procedure. First, the temperature inside the cloud chamber was varied in order to change the shape of ice crystals and was kept constant to maintain the same shape of ice crystals until one scat-

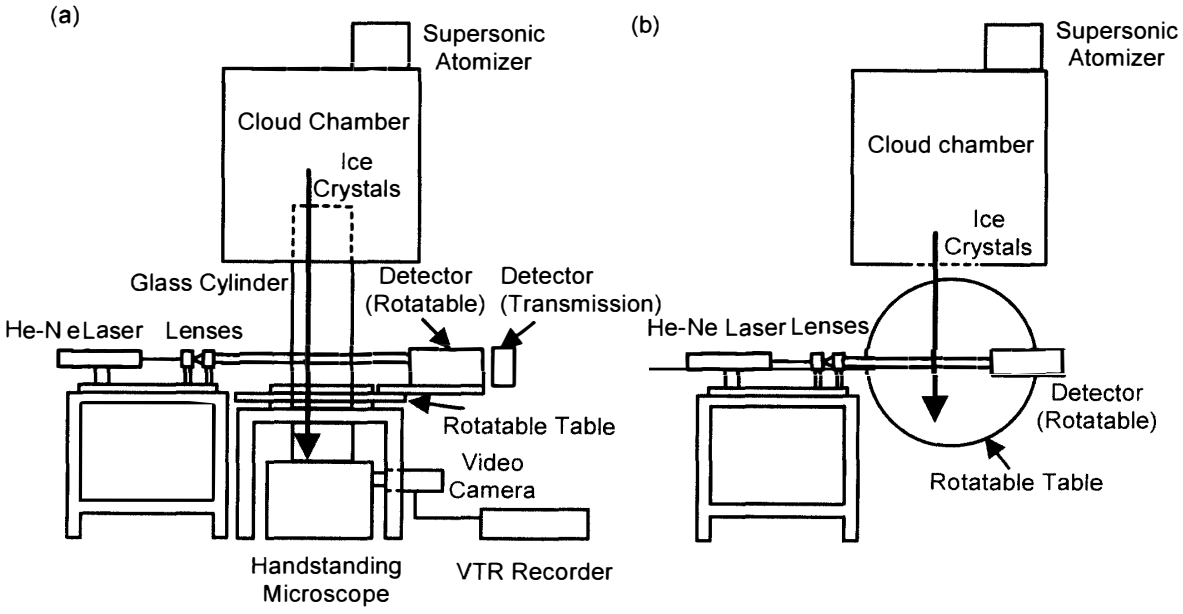

Fig. 1. Experimental apparatus for measurement of the scattering pattern in the horizontal scattering plane (a) and the vertical scattering plane (b).

tering pattern measurement was completed. Water droplets were then supplied into the cloud chamber by a supersonic atomizer. After a supercooled water cloud was generated inside the cloud chamber, the ice crystals were nucleated by the insertion of a chilled wire. The ice crystals started to grow in the cloud chamber, then fell into the glass cylinder, and finally fell on to the microscope stage at the bottom of the glass cylinder. Microscopic images of the ice crystals were recorded by a video camera and VTR system connected to the microscope. Through analysis of the video images, we were able to obtain information on the shapes, sizes and internal structures of the ice crystals. In this experiment, the sizes of ice crystals were measured by the maximum dimensions (*i.e.*, plate diameter for plates and *c*-axis length for columns). Moreover, spatial concentrations were measured by using the impactor replicator, which collected cloud samples by impaction onto a freshly Formvar solution-coated substrate in order to count the number of ice crystals per unit volume.

Furthermore, the scattering intensities of the laser beam in the horizontal scattering plane were measured. A collimated and unpolarized laser beam (He-Ne laser with a wavelength of 633 nm, power of 10 mW) was expanded to a ray of light with a diameter d of 1 cm and applied at the center of the glass cylinder. The incident ray was scattered by the ice crystals. The total intensity of light scattered by the ice crystals at the center of the glass cylinder was measured by a silicon photodiode combined with lenses and slits. Since the whole detector system was placed on a rotating table, the angular distribution of the scattering intensity (*i.e.*, the scattering pattern) could be measured. The scattering angle (θ) was measured from the direction of the incident light, and the scattering intensities were measured between 10° and 150° in order to prevent interaction with incident light in the vicinity of $\theta=0°$ or 180°. It should be noted that the glass cylinder did not affect the scattering pattern, because the detector system measures only the scattered light ray that crosses the glass cylinder perpendicularly. Another silicon photodiode mounted behind the laser beam exit point (*i.e.*, at $\theta=0°$) was used to monitor fluctuations in cloud composition that orig-

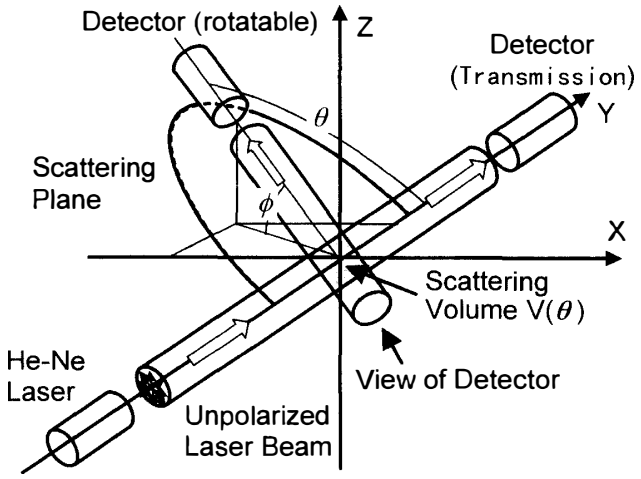

Fig. 2. Detailed optical system for measurement of the scattering pattern.

inated from the shape, size distribution and spatial concentration. Because the shape and size distributions of ice crystals were confirmed in a stable cloud condition by *in-situ* observation under the microscope, the fluctuation was due to the change of the spatial concentration in one whole scan, which took 2 min. Therefore, the record of the laser beam transmission through the cloud could be used to identify the stable cloud condition.

On the other hand, in order to measure the scattering pattern on the vertical scattering plane, the detecting system was rotated vertically, and both the glass cylinder and the microscope were removed, as shown in Fig. 1b. We used the same laser beam as an incident light source in the horizontal scattering plane. Moreover, the shapes and sizes of ice crystals were analyzed by the replicated image of ice crystals onto microscope slides coated with freshly Formvar solution.

2.2. Method of experimental analysis for the scattering pattern

The basic parameter of the experimental angular scattering pattern is the volume scattering coefficient $B(\theta, \phi)$ at the scattering angle θ and elevation angle ϕ of the scattering plane (see Fig. 2). $B(\theta, \phi)$ gives information on the angular distribution of scattered intensity from unit volume as a function of direction. In general, $B(\theta, \phi)$ can be derived from the following equation:

$$I(\theta, \phi) = V(\theta, \phi)\, B(\theta, \phi)\, I_0, \tag{1}$$

where $I(\theta, \phi)$ is the measured scattering intensity, $V(\theta, \phi)$ the scattering volume (m^3) and I_0 the intensity of incident light.

In this study, $B(\theta, \phi)$ was normalized by the scattering intensity at $\theta = 10°$ and $\phi = 0°$ in order to compare the scattering patterns for different physical properties of an ice cloud. It is desirable to express the results in the form of a relative scattering function $f(\theta, \phi)$, defined by

$$f(\theta, \phi) = \frac{B(\theta, \phi)}{B(10°, 0°)}. \tag{2}$$

Here, since the scattering volume is given by $16\, d^3/3 \sin\theta$, eq. (2) is simplified as

$$f(\theta, \phi) = \frac{I(\theta, \phi)}{I(10°, 0°)} \frac{\sin\theta}{\sin(10°)}. \tag{3}$$

Hereafter, the scattering patterns are discussed on the basis of the measured $f(\theta, \phi)$.

The extinction coefficient σ (m^{-1}) was used to monitor the fluctuations in the cloud. This value was obtained from the following equation:

$$\sigma = -\frac{1}{R} \ln \frac{I_e}{I_0}, \tag{4}$$

where R is the total cloud length, and I_e the light intensity of the laser light that traversed through the cloud.

3. Results and Discussion

3.1. Effect of crystal shape on the scattering pattern in the horizontal plane

Figure 3a and b indicate the size distribution of ice crystals and the scattering patterns, respectively. The solid and dotted lines show the results when the hexagonal solid columns (at a temperature of -7.5°C and $\sigma=0.71$ m^{-1}) and the hexagonal solid plates (at a temperature of -16.7°C and $\sigma=0.85$ m^{-1}) are observed dominantly in the falling crystals, respectively. Since the modal maximum dimensions are almost the same (20 μm for both cases (see Fig. 3a)), the difference in scattering patterns may be due to only the difference in ice crystal shapes. The spatial concentrations of

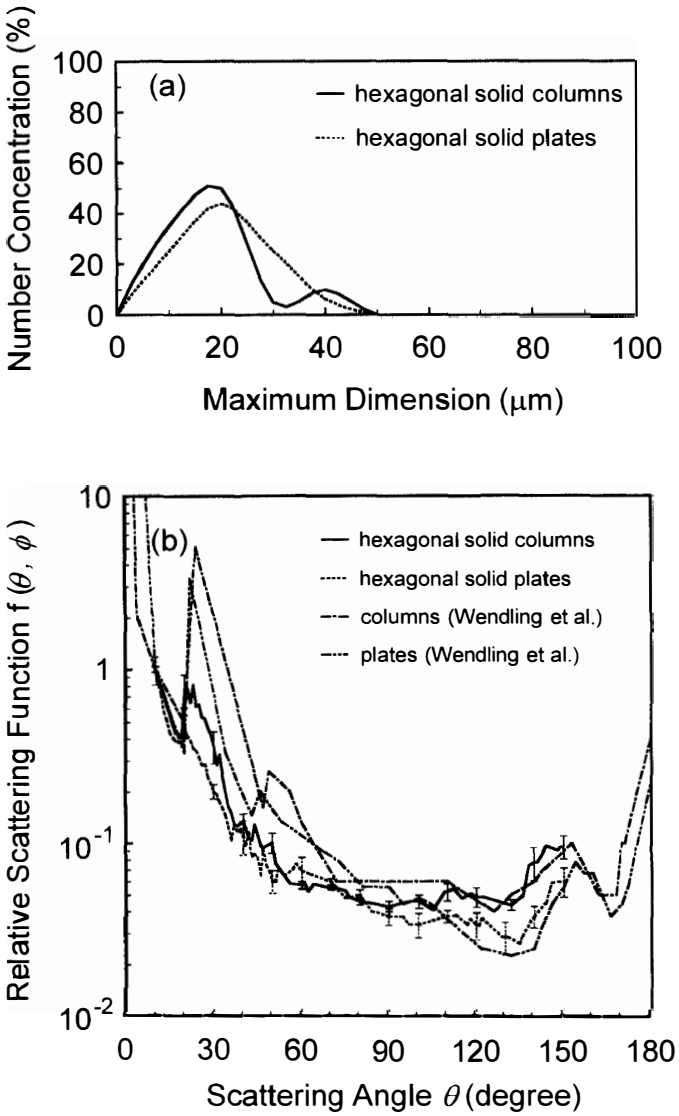

Fig. 3. Experimental results for an ice cloud composed of hexagonal solid columns (solid line) and hexagonal solid plates (dotted line). (a) The size distributions of ice crystals, (b) the scattering patterns obtained by laboratory experiment and by computer simulations (WENDLING et al., 1979)

the ice crystals were 98.5 (cm^{-3}) for the hexagonal solid columns and 122.3 (cm^{-3}) for the hexagonal solid plates.

The dependence of the scattering pattern on crystal shape derived from this experiment is summarized as follows. First, the peaks at the halo angle of 22°, which are caused by minimum deviation of light through the 60° prism, were observed for both cases. However, the intensity in the case of hexagonal solid columns was much stronger than in the case of hexagonal solid plates. This is due to the difference in the area on the prism faces between the hexagonal solid columns and the hexagonal solid plates. Second, the scattering intensities increase at scattering angles above 150° for both types. These increases correspond to the backscattering peak. However, the intensity for the hexagonal solid columns was also stronger than that for the hexagonal solid plates. Third, the sidescattering intensity measured for the hexagonal solid columns was stronger than those for the hexagonal solid plates.

The differences in the backscattering and the sidescattering are explained as follows. By means of computer simulation for randomly oriented hexagonal columns, CAI and LIOU (1982) and MACKE (1993) showed that the backscattering and sidescattering are caused by internal reflections rather than external reflections. On the other hand, WENDLING *et al.* (1979) showed that the basal planes confine the light rays to penetrate them, and contribute to the forward scattering for randomly oriented ice crystals. Consequently, the prism faces mainly contribute to the backscattering and sidescattering in the case of randomly oriented ice crystals. In this experiment, ice crystals prefer to oscillate, and each ice crystal had a different fall orientation (FRASER, 1979). Therefore, hexagonal solid columns, of which prism faces have a larger area than that of hexagonal solid plates with the same maximum dimension, contribute more to backscattering and sidescattering than do hexagonal solid plates.

Figure 3b also shows results calculated by computer simulation (WENDLING *et al.*, 1979), which used a wavelength of 0.55 μm as incident light, and calculated for hexagonal solid columns with maximum dimension of 480 μm and for hexagonal solid plates with maximum dimension of 500 μm. The results calculated by computer simulations were normalized to unity at a scattering angle of 10°. A comparison between this experiment and the computer simulation shows that there was general agreement, although it is not possible to carry out a precise comparison because our data lacked values within 10° of forward and backscattering direction ($\theta > 150°$) due to the limitations of the optical system.

On the other hand, we also observed scattering patterns for ice crystals with more complicated shapes. Figure 4b shows an example of a scattering pattern for columnar crystals with pyramidal faces (solid line, at a temperature of −7.0°C and spatial concentration of 94.2 (cm^{-3})), as shown in Fig. 4a. The extinction coefficient in this experiment was $\sigma = 0.75$ m^{-1} and was almost constant until the scattering pattern measurement was completed. To compare this result with the scattering pattern for a hexagonal solid column, the scattering pattern for the hexagonal solid column (dotted line), which has shown in Fig. 3b, is also shown. In this case, the modal maximum size is 20 μm. A peak at $\theta = 18°$, which corresponds to a 18° halo, is observed in addition to the 22° peak. This peak is produced by rays transmitted through one pyramidal face and then the opposite pyramidal face (GOLDIE *et al.*, 1976).

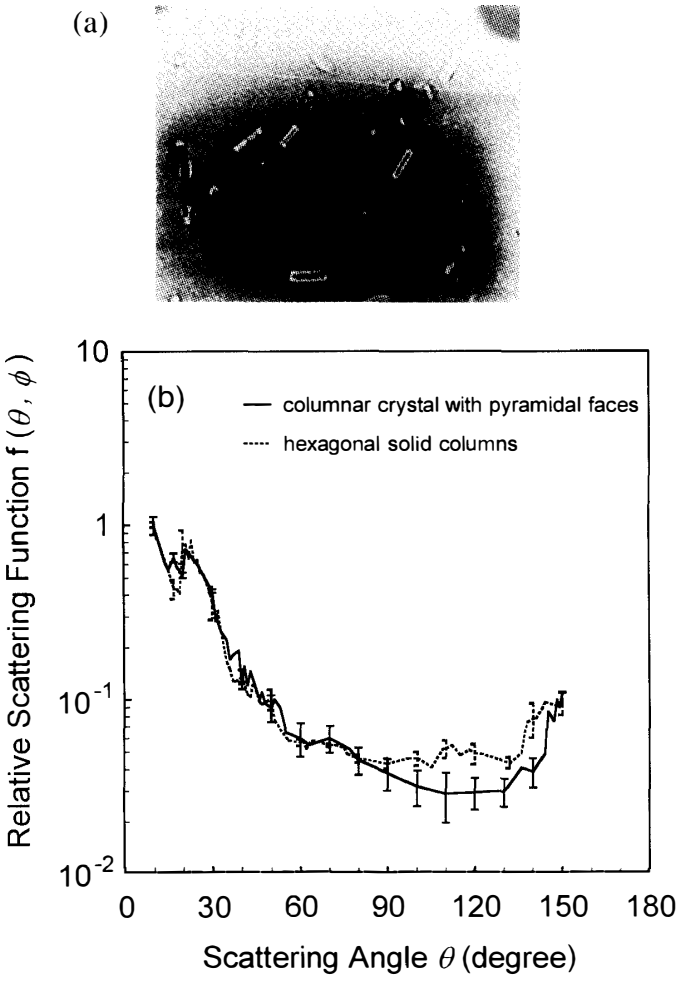

Fig. 4. Experimental results for an ice cloud composed of columnar ice crystals with pyramidal faces (solid line). The results for an ice cloud composed of hexagonal solid columns are also shown by the dotted line, which is the same as the one shown in Fig. 3b. (a) A microphotograph of the columnar crystals with pyramidal faces, which is a reversed image to clearly show the shape of ice crystals. (b) The scattering patterns.

Figure 5b shows an example of a scattering pattern for sector plates (solid line, at a temperature -14.4°C and spatial concentration of 110.2 (cm^{-3})), as shown in Fig. 5a. The extinction coefficient is $\sigma=0.82$ m^{-1} and is almost constant during one whole scan. The same pattern (dotted line) as that has already shown in Fig. 3b is shown again in this figure to compare this result with that for hexagonal solid plates. Although a 22° peak is not observed when the sector plates are dominant, the intensity of the forward scattering (θ <50°) is slightly stronger than the intensities for the hexagonal solid plates. The reason why the scattering pattern has no peak is that the sector branches prevent a 60° prism from being made, which causes a 22° halo. Moreover, a branch of the sector plates intensifies the forward scattering by producing two refractions through the branch.

Two results on the irregular shaped crystals show that the existence of high-indexed faces of crystals, such as pyramidal faces and branch of a sector plate, affects

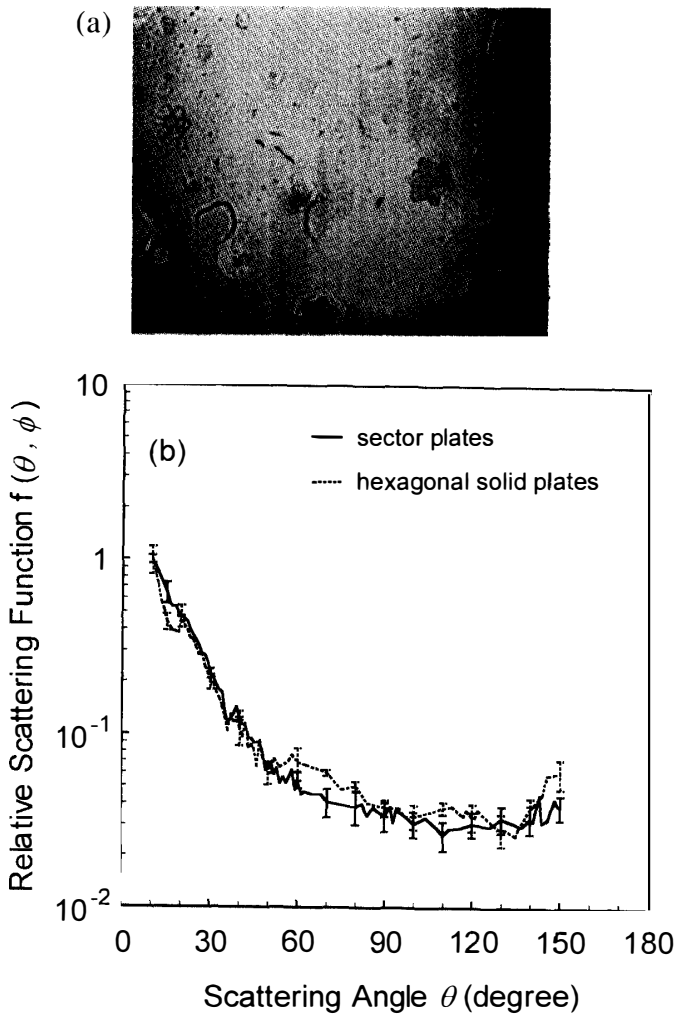

Fig. 5. Experimental results for an ice clouds composed of sector plates (solid line). The results for an ice cloud composed of hexagonal solid plates is also shown by the dotted line, which is the same as the one shown in Fig. 3b. (a) A microphotograph of sector plates. (b) The scattering patterns.

the scattering patterns, especially in the forward direction.

3.2. Scattering pattern in a vertical scattering plane

The scattering patterns were also measured in a vertical plane. Figure 6 shows the results of a scattering pattern in a vertical scattering plane (solid line), which were obtained for a cloud composed of hexagonal solid plates with a modal size of 20 μm. The dotted line also indicates the scattering pattern in a horizontal plane, which is the same as that shown in Fig. 3b. Although the extinction coefficient was not measured in a vertical scattering plane, the cloud condition in one whole measurement in a vertical scattering plane was in a steady state because the measurement was carried out in 2 min, which was the same as that in a horizontal scattering plane. In this study, we show the difference of the scattering patterns between vertical and horizontal scattering planes.

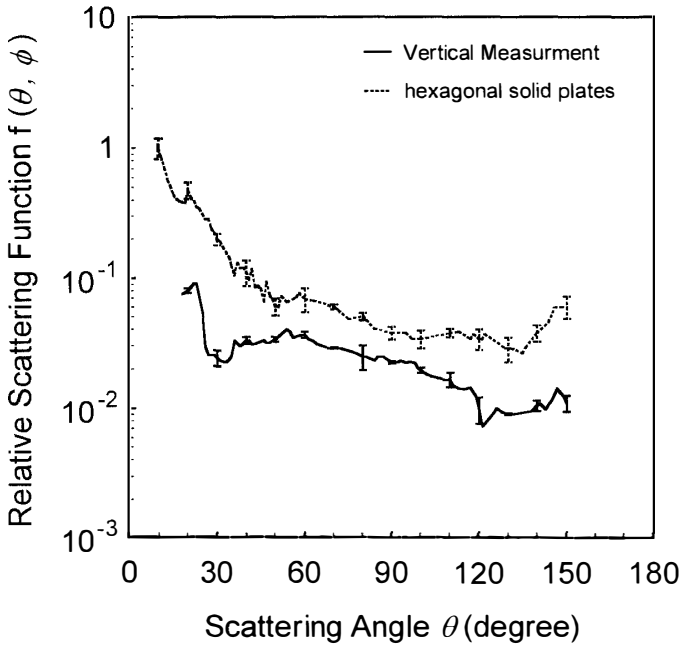

Fig. 6. Scattering pattern measured in the vertical scattering plane. The solid line shows the results for hexagonal solid plates with a modal size of 20 μm. The dotted line shows the scattering pattern for an ice cloud composed of the hexagonal solid plates (the same as that shown in Fig. 3) for a comparison of horizontal and vertical scattering planes.

The scattering pattern in the vertical scattering plane is completely different from that in the horizontal scattering plane in qualitatively. A sub peak is characteristically observed at $\theta=50^\circ$, and also the effect of backscattering is not clear in the vertical plane. The scattering pattern observed in the vertical plane may be caused by the fall orientation of the ice crystals. As mentioned previously, ice crystals with a size of 20 μm or more prefer to oscillate within the tip angle of about 20° in the stationary state air (FRASER, 1979). In our experiment, the tip angle should be larger than the angle calculated by FRASER because of convection in the glass cylinder. If the average tip angle exceeds 25° by convection, external reflection may contribute to form the sub peak. Moreover, the prism faces do not contribute effectively to backscattering in the vertical plane because they do not face the vertical direction.

4. Conclusions

Measurements of scattering patterns were successfully carried out as a function of the physical properties of ice crystals.

We measured the scattering patterns for hexagonal solid columns, hexagonal solid plates, columns with pyramidal faces, and sector plates. It was demonstrated that scattering patterns for different shapes of ice crystals are significantly different. Especially, irregular shaped ice crystals produced completely different patterns from those for hexagonal solid crystals. We also measured the scattering pattern in the vertical scattering plane for hexagonal solid plates. It was successfully demonstrated that there is

large anisotropy of the scattering patterns depending on the scattering planes. Further study is needed to clarify the 3-dimensional scattering pattern of an ice cloud.

In this study, we showed that the experimental method is a good way to clarify the relationships between scattering properties and ice crystal shapes. However, there are other physical properties of ice clouds, such as size distribution, spatial concentration, falling orientation, and so on. We will study the dependencies of scattering patterns on these physical properties using our method in the future. The relationships between polarimetric properties and physical properties of ice crystals will also be studied.

Acknowledgments

One of the authors (Y. F) thanks Prof. J. HALLETT for leading him to this research field. This work was partially supported by the Inamori Foundation, and by Grant-in-Aid for Scientific Research (A) No. 07404050 from the Ministry of Education, Science, Sports and Culture, Japan.

References

CAI, Q. and LIOU, K. N. (1982): Polarized light scattering by hexagonal ice crystals: Theory. Appl. Opt., **21**, 3569–3580.

FRASER, A. B. (1979): What size of ice crystals causes the halos? J. Opt. Soc. Am., **69**, 1112–1118.

GOLDIE, E. C. W, MEADEN, G. T. and WHITE, R. (1976): The concentric halo display of 14 April 1974. Weather, **31**, 304–312.

HEYMSFIELD, A. J. (1975): Cirrus uncinus generating cells and the evolution of cirriform couds part I: Aircraft observation of growth of ice phase. J. Amos. Sci., **32**, 799–808.

HEYMSFIELD, A. J. and KNOLLENBERG, R. G. (1972): Properties of cirrus generating cells. J. Atmos. Sci., **29**, 1358–1366.

LIOU, K. N. (1992): Radiation and Cloud Processes in the Atmosphere: Theory, Observation, and Modeling. New York, Oxford Univ. Press, 487 p.

MACKE, A. (1993): Scattering of light by polyhedral ice crystals. Appl. Opt., **32**, 2780–2788.

MORITA, Y. (1973): Scattering cross section for the visible light by the levitated ice crystals. Tenki, **20**, 13–22 (in Japanese).

NIKIFORVA, N. K., PAVLOVA, L. N., PETRUSHIN, A. G., SNYKOV, V. P. and VOLKOVITSKY, O. A. (1977): Aerodynamic and optical properties of ice crystals. J. Aerosol. Sci., **8**, 243–250.

ROCKWITZ, K. D. (1989): Scattering properties of horizontal oriented ice crystal columns in cirrus clouds. Part I. Appl. Opt., **28**, 4035–4250.

SASSEN, K. and LIOU, K. N. (1979a): Scattering of polarized laser light by water droplet, mixed-phased and ice crystal clouds. Part I: Angular scattering patterns. J. Atmos. Sci., **36**, 838–851.

SASSEN, K. and LIOU, K. N. (1979b): Scattering of polarized laser light by water droplet, mixed-phased and ice crystal clouds. Part II: Angular depolarizing and multiple-scattering behavior. J. Atmos. Sci., **36**, 852–861.

TAKANO, Y. and LIOU, K. N. (1989a): Solar radiative transfer in cirrus clouds. Part I: Single-scattering and optical properties of hexagonal ice crystals. J. Atmos. Sci., **46**, 3–19.

TAKANO, Y. and LIOU, K. N. (1989b): Solar radiative transfer in cirrus clouds. Part II: Theory and comparison of multiple scattering in an anisotropic medium. J. Atmos. Sci., **46**, 20–36.

TAKANO, Y. and LIOU, K. N. (1995): Radiative transfer in cirrus clouds. Part III: Light scattering by irregular ice crystals. J. Atmos. Sci., **52**, 818–837.

WENDLING, P., WENDLING, R. and WEICKMANN, H. K. (1979): Scattering of solar radiation by hexagonal ice crystals. Appl. Opt., **18**, 2663–2671.

(Received February 16, 1998; Revised manuscript accepted May 26, 1998)